Hindawi Publishing Corporation
International Journal of Photochemistry
Volume 2014, Article ID 387536, 6 pages
http://dx.doi.org/10.1155/2014/387536

Research Article

The Photocatalytic Oxidation of 4-Chlorophenol Using Bi_2WO_6 under Solar Light Irradiation

Lorean Madriz,[1] José Tatá,[1] and Ronald Vargas[2]

[1] *Department of Chemistry, Organic Analysis and Catalysis Laboratory, Simón Bolívar University, Caracas 1080A, Venezuela*
[2] *Department of Chemistry, Electrochemistry Laboratory, Simón Bolívar University, Caracas 1080A, Venezuela*

Correspondence should be addressed to Lorean Madriz; lmadriz@usb.ve

Received 30 April 2014; Accepted 28 June 2014; Published 5 August 2014

Academic Editor: M. El-Khouly

This report discusses the effects of the initial concentration of 4-chlorophenol (4-CP) on its solar light photoinduced oxidation/mineralization kinetics on Bi_2WO_6 catalyst. Photocatalytic degradation followed the Langmuir-Hinshelwood (L-H) mechanism. From the kinetic data the Langmuir adsorption equilibrium constant of 4-CP on the Bi_2WO_6 surface and the L-H maximum reaction rate for 4-CP oxidation have been evaluated. Chromatographic and spectroscopy studies show the presence of *p*-benzoquinone and maleic acid as the main reaction products; these compounds first increase and then decay until they disappear. Chemical oxygen demand (COD) and produced CO_2 measurement show that photocatalytic mineralization of the phenolic compound was readily possible in a wide concentration range.

1. Introduction

In recent years, a large number of investigations have focused on the development of visible light induced heterogeneous photocatalyst for its applications in solar energy conversion and environmental wastewater purification [1–4]. In this sense, efforts have been directed to developing nanostructures based on Bi_2WO_6, the simplest member in the Aurivillius family [5–10]. This compound was first studied by Kudo and Hijii [11] and Zou and coworkers [12]; their works revealed that Bi_2WO_6 could perform as an excellent photocatalytic material, because it presents enhanced activities for the oxidative water splitting reaction. As a result, the solar light photocatalytic degradation of many pollutants as rhodamine B [13], green malachite [14], benzene [15], and 2,4-dichlorofenoxiacetic acid (2,4-D) [16] has been studied.

The photoinduced degradation of 4-chlorophenol (a water soluble hazardous material widely used in paper, pharmaceutical, pesticide, and coal industries) [17–19] with Bi_2WO_6 nanocatalysts under visible light irradiation has been tested [20, 21]. This method induces an important decrease in the organic load and toxicity of wastewater; however, these authors have considered that the photodegradation reaction follows first order kinetics [22], thus obtaining the overall oxidation rate constant from linear plots of $\ln(c_{(t)}/c_0)$ versus t. Nonetheless, this constant does not describe each of the steps of the overall reaction mechanism; hence, its value will depend in general on the detailed conditions under which the experiments are carried out. However, less effort has been expended on measuring the kinetic parameters of environmental pollutant degradation and mineralization according to a heterogeneous catalysis model like Langmuir-Hinshelwood kinetics. Knowledge of these parameters permits investigators to establish the reaction mechanisms and optimal reaction conditions needed to properly describe the process for use in designing chemical reactors at large scales.

In the present work, we discuss the kinetics of 4-CP solar light photoinduced oxidation/mineralization kinetics on Bi_2WO_6 catalyst. Our results show that mineralization kinetics of this phenolic compound is determined by their surface concentration according to the Langmuir-Hinshelwood mechanism. The kinetic parameters of this model are reported and mechanistic implications are discussed.

2. Material and Methods

2.1. Materials. The following reactants were used without further purification: 4-chlorophenol, C_6H_5OCl, 99%, Merck; bismuth (III) nitrate pentahydrate, $Bi(NO_3)_3{\cdot}5H_2O$, 99%, Merck; sodium tungstate dihydrate, $Na_2WO_4{\cdot}2H_2O$, 99%, Riedel de Häen; titanium dioxide, TiO_2, Anatase, Riedel de Haën; potassium monobasic phosphoric acid, KH_2PO_4, 99%, Riedel de Haën; potassium dibasic phosphoric acid, K_2HPO_4, 98%, Riedel de Haën; potassium phosphate $K_3PO_4{\cdot}H_2O$, 95%, Riedel de Haën; sulfuric acid, H_2SO_4, 95–97%, Riedel de Haën; potassium dichromate, $K_2Cr_2O_7$, 99.5%, Merck; potassium hydrogen phthalate, $C_8H_5KO_4$, 99.5%, Riedel de Haën; mercury (II) sulfate, $HgSO_4$, ≥99%, Merck; silver sulfate, Ag_2SO_4, ≥99%, Merck; water, H_2O, 17.7 MΩ/cm, Nanopure.

2.2. Equipment. A Solar Light Co. solar light simulator with a 1000 W xenon lamp and the appropriate filters for producing solar light (290–900 nm) was used in the experiments. Solar light radiometer and Ocean Optics fiber optic spectrometer model S1024dw were used to determine the radiation intensity and simulated spectra during each trial. Solutions pH was recorded using a digital pH-meter, model P211, Hanna Instruments. Millipore filtration equipment with 0.05 μm membrane filters was used to separate the photocatalyst from the sample solutions. A diode arrangement UV-Vis spectrophotometer by Hewlett Packard (model HP8452A) was used to obtain the 4-CP UV-Vis spectrum. Waters Association HPLC with model M6000A pump, Rheodyne injector, model 484 UV detector, and model 745B data recorder was used to identify the intermediates formed during the reaction.

2.3. Methods

2.3.1. Synthesis and Characterization of the Bi_2WO_6 Photocatalyst. Bi_2WO_6 nanocrystals were fabricated according to the widely reported hydrothermal synthesis [6, 7, 13, 14, 23, 24]. As a typical process, aqueous solutions of $Na_2WO_4{\cdot}2H_2O$ (5 mM) and $Bi(NO_3)_3{\cdot}5H_2O$ (10 mM) were mixed together (maintained the 1 : 2 molar ratio) until they reached 200 mL. White precipitate appeared immediately and was put in ultrasonic bath for 10 min in order to complete the precipitation. The solution pH was adjusted to 7.0 and the final solution was added into a 300 mL stainless steel Parr autoclave; the experimental conditions were established in 160°C and 70 psig for 24 h. Then, the reactor was cooled to room-temperature naturally; the resulting sample was collected and washed with deionized water. Finally, the obtained powder was dried at 80°C in air.

The characterization of the obtained photocatalyst according to the described procedure has been reported by our group; for details see [10, 25, 26]. The main results for the Bi_2WO_6 powder are nanocrystals with orthorhombic phase, semiconductor band gap energy of 2.55 eV, B.E.T. specific surface area of 48 m^2/g, and internal pore diameter of 7 nm. These values are typically reported for the highly active bismuth tungstate photocatalytic materials [6, 7, 10, 13, 14, 23–26].

2.3.2. Photocatalytic Oxidation of 4-Chlorophenol Using Bi_2WO_6 under Solar Light Irradiation. The photocatalytic probes for 4-CP degradation were evaluated in a well-mixed batch configuration. In a beaker of 600 mL with magnetic agitation, a suspension of 500 mL of 4-CP and phosphate buffer solution (pH = 7) with 100 mg L^{-1} of the Bi_2WO_6 photocatalyst was prepared. This suspension remained in the dark for 30 min in order to establish the reactant-Bi_2WO_6 adsorption/desorption equilibrium. After this time, the system was placed under solar simulator cannon (diameter ca. 20 cm) in such a way that the distance between the end of the cannon and the beaker was 15 cm. The simulator was turned on, and the reaction was monitored by taking aliquots (3 mL) at different times. The aliquots were filtered with Millipore membranes, and the UV-Vis spectrum of the filtered solution was recorded. 4-CP analytical quantification was performed with the UV-Vis spectroscopy. The UV-Vis spectra obtained for the multicomponent solution (reactant + products) were deconvoluted using Matlab v 7.0 software, and the concentrations of the different compounds present in solution were determined according to the Lambert-Beer law, with molar absorption coefficients at the wavelengths of maximum absorption for each compound [27]. Simulator radiation was measured with a radiometer. Values of 100(±5) mW cm^{-2} were typically measured for solar visible radiation. The temperature of the reactor was kept at 22(±1)°C by maintaining the temperature of the room where the simulator was located.

2.3.3. Mineralization. Mineralization during 4-CP photocatalytic oxidation was followed by measuring the chemical oxygen demand (COD). In a typical reaction, aliquots (3 mL) were taken at different reaction times and the COD of each aliquot was measured with a colorimetric method [28, 29] in which the total organic sample content was oxidized for 2 h at 150°C in a closed system with sulfuric acid and potassium dichromate. The solution absorbance at 420 and 600 nm was then measured. From this absorbance, the solution COD was obtained from a potassium hydrogen phthalate calibration curve. Mineralization was confirmed by direct CO_2 measurement using an OxyGuard portable dissolved CO_2 analyzer based on nondispersive infrared spectrometry (NDIR).

2.3.4. HPLC Studies. Liquid chromatography was carried out with a Waters Association HPLC system composed of a model M6000A pump, a Rheodyne injector, a model 484 UV detector, and a model 745B data recorder. A μ Bondapack CN (RP) 3.9 mm × 150 mm column was used to determine the intermediaries, with 70/30 water/methanol solution as mobile phase, at 0.9 mL/min flow rate and 254 nm UV-Vis detection. Maleic acid was analysed with an Aminex HPX-87, 7.8 mm × 300 mm column, using 8×10^{-4} M sulphuric acid aqueous solution as mobile phase at 0.5 mL/min flow rate, with detection at 210 nm.

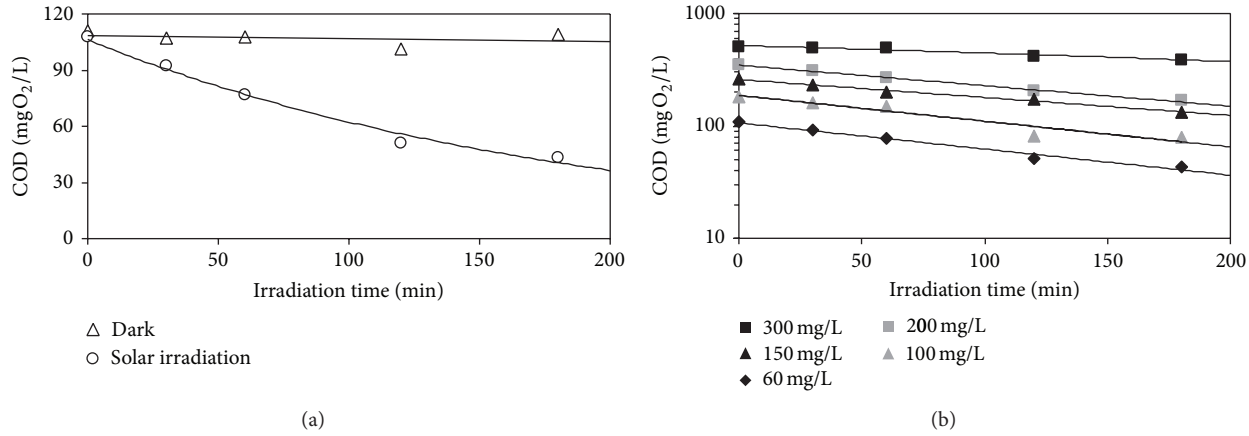

Figure 1: (a) COD diminution during the photocatalytic oxidation of the 4-CP on Bi_2WO_6. (b) Effect of the initial concentration of 4-CP on COD diminution during the visible light photocatalytic oxidation of the 4-CP on Bi_2WO_6. (—) Pseudo first order kinetics decay.

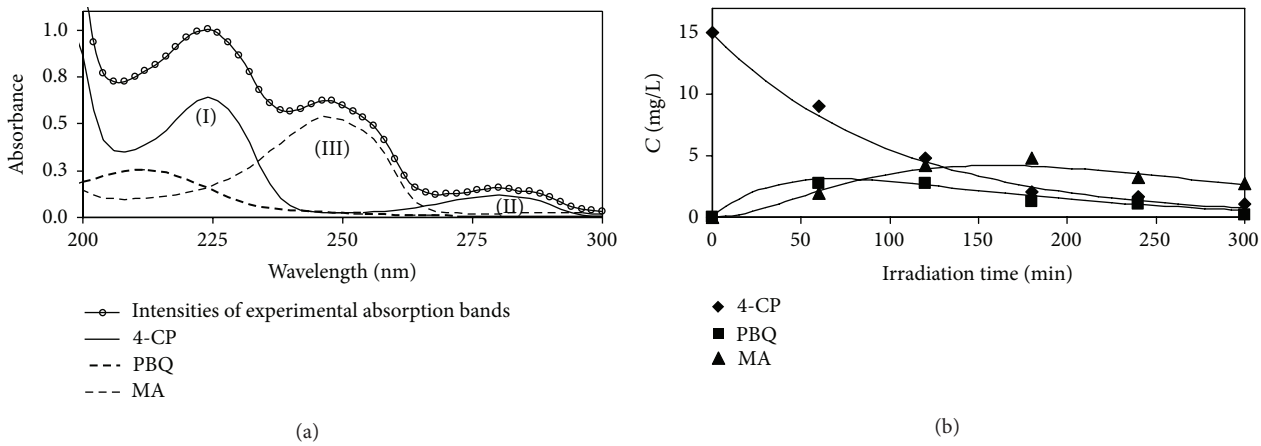

Figure 2: (a) Deconvoluted UV-Vis spectra of 15 ppm of 4-CP, after 30 min of solar light irradiation in presence of 100 mg/L of Bi_2WO_6 at neutral pH. Intensities of deconvoluted absorption bands ((—) 4-CP, (- - -) PBQ, and (– – –) MA). (b) Concentration versus irradiation time curves during the 4-CP degradation.

3. Results and Discussion

Figure 1(a) shows that the degradation of 4-CP on Bi_2WO_6 under solar irradiation is able to generate a dramatic COD diminution of the wastewater. The total COD diminution implies that efficient conversion to CO_2 occurred during solar irradiation. This result was confirmed by the direct measurement by NDIR of the CO_2 produced during 30 mg L^{-1} of 4-CP photocatalytic oxidation; the final concentration of dissolved carbon dioxide (1.1 ± 0.2 mM) corresponds very well with the predicted stoichiometrically assuming that all 4-CP was oxidized completely (1.4 mM). It should be noted that COD remains a constant value when the suspension is in the dark. Figure 1(b) shows the influence of the initial concentration of 4-CP on the diminution of the COD. It should be noted that the COD decrease is assessment in a wide range for the initial quantity of organic compound and follows a pseudo first order kinetic decay.

Figure 2(a) shows deconvoluted UV-Vis spectra of 15 ppm of 4-CP, after 30 min of solar light irradiation in presence of 100 ppm of Bi_2WO_6 at neutral pH. It should be noted that the bands between 200–240 nm (I) and 260–300 nm (II) are associated with the starting compound, and the 4-CP absorption band with its maximum at 280 nm decreases continuously with the irradiation time. The band between 225 and 260 nm (III) increases as 4-CP is oxidized. This band arises from the oxidation of the phenolic compound to a *p*-benzoquinone compound. This has been reported as the principal reaction intermediate during oxidation of several phenolic compounds [27, 30, 31] and was verified with high performance liquid chromatography (HPLC). In general, the chromatographic and spectroscopy analysis indicated that the more stable intermediaries observed during the photooxidation of 4-CP are the *p*-benzoquinone (PBQ) and the maleic acid (MA), where in all intermediaries there was an increase in concentration at first and then they decreased until they disappeared (see Figure 2(b)). It should be noted that these compounds are the main intermediates reported during the reaction between 4-CP and hydroxyl radicals in other advanced photooxidation process like TiO_2/UV [27, 31,

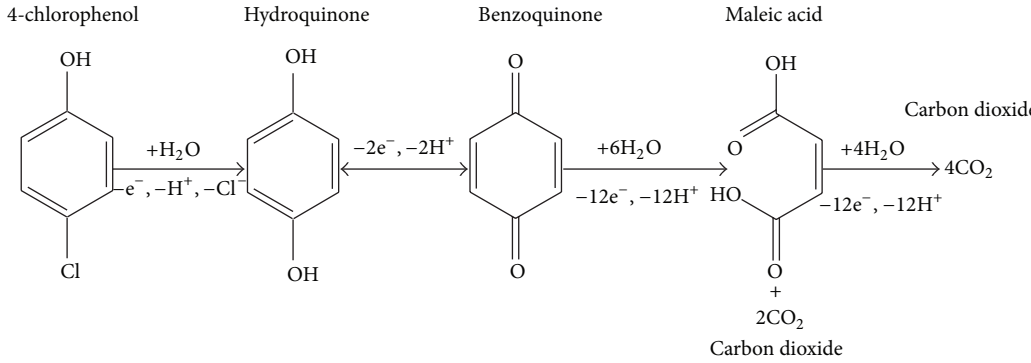

Scheme 1: Principal reaction pathways (intermediates detected) during the 4-CP oxidation after the consecutive hydroxyl radicals attack.

32]. However, these intermediates have UV spectra; therefore, to obtain the 4-CP concentration a determination involving numerical deconvolution of the spectra data according to the Lambert-Beer law for multicomponent mixtures is required [27]. Figure 2(b) showed the result obtained for the photocatalytic oxidation of 4-CP. The concentration of the initial compound decreases continuously until it reaches low values, and the concentration of the more stable intermediates (PBQ and MA) first increases and then decays.

Chromatographic and spectroscopy studies show that the mechanism of oxidative mineralization of phenolic compounds involves first the formation of highly toxic quinones and then the subsequent opening of the aromatic rings leading to formation of aliphatic acids and finally to carbon dioxide [27, 30, 31]. In Scheme 1, the principal oxidation reaction pathways (intermediates detected) during the 4-CP oxidation after the consecutive hydroxyl radicals attack are shown. However, chemical analysis indicated that at large irradiation time this intermediate is not accumulated leading to the completed mineralization of the initial 4-CP in solution.

According to many researchers [31, 33–38], the influence of the initial concentration of the solute on the photocatalytic degradation rate of the most organic compounds is described by the Langmuir-Hinshelwood model

$$r = \frac{kKC}{\left(1 + KC + \sum K_i C_i\right)}, \tag{1}$$

where r (mg L^{-1} min^{-1}) is the reaction rate of disappearance of 4-CP, C (mg L^{-1}) is the concentration of the organic compound, K (L mg^{-1}) represents the equilibrium adsorption constant of the organic compound on the photocatalyst, and k (mg L^{-1} min^{-1}) reflects the limiting reaction rate at maximum coverage for the experimental conditions. In this case the 4-CP adsorbs fast at the Bi_2WO_6 and then reacts consecutively with the $OH^{\bullet}$, in order to produce the p-hydroquinone (PHQ), PBQ, MA, and finally CO_2. As pointed out [35], the initial rate method should be used to validate the kinetic model, with assumption of no competition with reaction byproducts, because when $t \rightarrow 0$, it results in $\sum K_i C_i \ll 1 + K_{4\text{-CP}} C_{4\text{-CP}}$. Then the simplest representation

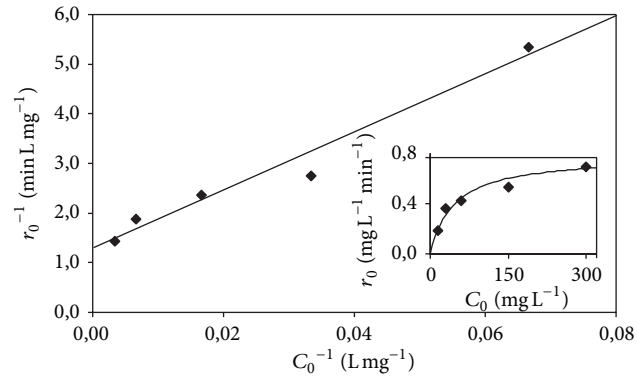

Figure 3: Langmuir-Hinshelwood kinetic linear representation of the solar light photooxidation/mineralization of 4-CP on Bi_2WO_6. Inset: graphical representation of the L-H model. (♦) Experimental data and (—) equation (1) with $k = 0.78$ mg L^{-1} min^{-1}, $K = 0.02$ L mg^{-1}.

for the initial rate of disappearance of 4-CP on Bi_2WO_6 is given by

$$r_0 = \frac{kKC_0}{\left(1 + KC_0\right)}. \tag{2}$$

The r_0 were determined by linear fit from the 4-CP concentration versus irradiation time curves at the initial times; then the L-H model was verified according to the linear representation of (2); that is, a plot of the inverse initial rate ($1/r_0$) as a function of the inverse initial concentration ($1/C_0$) should be linear.

As indicated in Figure 3, the $1/r_0$ versus $1/C_0$ plot yields a straight line. From the linear fit the L-H kinetic constants for the 4-CP photooxidation using Bi_2WO_6 under solar light irradiation are $k = 0.78$ mg L^{-1} min^{-1} and $K = 0.02$ L mg^{-1}. In order to compare the kinetic efficiency of this system, the maximum value for the first order kinetic constant ($k_{obs} = kK$) was estimated (for L-H model $k_{obs} = kK/(1 + KC)$ and if $KC \ll 1$, the maximum k_{obs} becomes kK) [35]. In this work we find $k_{obs} = 0.02$ min^{-1} for 4-CP on Bi_2WO_6 + solar light and Theurich and coworkers report $k_{obs} = 0.08$ min^{-1} for 4-CP on TiO_2 + UV light [31]. It

should be noted that the catalytic efficiency observed in Bi_2WO_6/solar light degradation of 4-chlorophenol is slightly lower but in the same order of magnitude for the well-known TiO_2/UV advanced oxidation process. Therefore, the use of solar light makes the Bi_2WO_6 a promising material towards the decontamination of polluted water.

4. Conclusions

Photocatalytic degradation of 4-chlorophenol (4-CP) on Bi_2WO_6 under solar irradiation followed the Langmuir-Hinshelwood mechanism; the respective kinetic constants are $k = 0.78\,\text{mg}\,\text{L}^{-1}\,\text{min}^{-1}$ and $K = 0.02\,\text{L}\,\text{mg}^{-1}$. Studies performed by several techniques show the presence of *p*-benzoquinone and maleic acid as the main reaction products; these compounds disappear to form carbon dioxide. Chemical oxygen demand and produced CO_2 measurements show that photocatalytic mineralization of the phenolic compound was readily possible in a wide concentration range. The results obtained for the solar light photoinduced oxidation/mineralization of 4-chlorophenol on Bi_2WO_6 catalyst demonstrate the use of this semiconductor as material potential for decontamination of polluted water take advantage of solar energy.

Conflict of Interests

The authors declare that there is no conflict of interests regarding the publication of this paper.

Acknowledgment

The authors are grateful for the members of the Electrochemistry Group at Universidad Simón Bolívar for discussions.

References

[1] Q. Huang, S. Zhang, C. Cai, and B. Zhou, "β- and α-Bi2O3 nanoparticles synthesized via microwave-assisted method and their photocatalytic activity towards the degradation of rhodamine B," *Materials Letters*, vol. 65, no. 6, pp. 988–990, 2011.

[2] J. Bandara, J. A. Mielczarski, A. Lopez, and J. Kiwi, "Adsorption mechanism of chlorophenols on iron oxides, titanium oxide and aluminum oxide as detected by infrared spectroscopy. Sensitized degradation of chlorophenols on iron oxides induced by visible light—comparison with titanium oxide," *Applied Catalysis B: Environmental*, vol. 34, pp. 321–333, 2001.

[3] D. Monllor-Satoca, L. Borja, A. Rodes, R. Gómez, and P. Salvador, "Photoelectrochemical behavior of nanostructured WO_3 thin-film electrodes: the oxidation of formic acid," *ChemPhysChem*, vol. 7, no. 12, pp. 2540–2551, 2006.

[4] C. Santato, M. Odziemkowski, M. Ulmann, and J. Augustynski, "Crystallographically oriented mesoporous WO3 films: synthesis, characterization, and applications," *Journal of the American Chemical Society*, vol. 123, no. 43, pp. 10639–10649, 2001.

[5] C. Xu, X. Wei, Z. Ren et al., "Solvothermal preparation of Bi_2WO_6 nanocrystals with improved visible light photocatalytic activity," *Materials Letters*, vol. 63, no. 26, pp. 2194–2197, 2009.

[6] M. Shang, W. Wang, S. Sun, L. Zhou, and L. Zhang, "Bi_2WO_6 nanocrystals with high photocatalytic activities under visible light," *The Journal of Physical Chemistry*, vol. 112, pp. 10407–10411, 2008.

[7] L. Zhang and Y. Zhu, "A review of controllable synthesis and enhancement of performances of bismuth tungstate visible-light-driven photocatalysts," *Catalysis Science and Technology*, vol. 2, no. 4, pp. 694–706, 2012.

[8] R. W. Wolfe, R. E. Newnahm, and M. I. Kay, "Crystal structure of Bi_2WO_6," *Solid State Communications*, vol. 7, no. 24, pp. 1797–1801, 1969.

[9] T. Saison, P. Gras, N. Chemin et al., "New insights into Bi_2WO_6 properties as a visible-light photocatalyst," *The Journal of Physical Chemistry*, vol. 117, no. 44, pp. 22656–22666, 2013.

[10] L. Madriz, J. Tatá, V. Cuartas, A. Cuéllar, and R. Vargas, "Celdas solares fotoelectroquímicas basadas en Bi_2WO_6," *Quimica Nova*, vol. 37, no. 2, pp. 226–231, 2014.

[11] A. Kudo and S. Hijii, "H2 or O2 evolution from aqueous solutions on layered oxide photocatalysts consisting of Bi3+ with 6s2 configuration and d0 transition metal ions," *Chemistry Letters*, no. 10, pp. 1103–1104, 1999.

[12] Z. Zou, J. Ye, K. Sayama, and H. Arakawa, "Direct splitting of water under visible light irradiation with an oxide semiconductor photocatalyst," *Nature*, vol. 414, no. 6864, pp. 625–627, 2001.

[13] C. Zhang and Y. Zhu, "Synthesis of square Bi2WO6 nanoplates as high-activity visible-light-driven photocatalysts," *Chemistry of Materials*, vol. 17, no. 13, pp. 3537–3545, 2005.

[14] Y. Chen, Y. Zhang, C. Liu, A. Lu, and W. Zhang, "Photodegradation of malachite green by nanostructured Bi_2WO_6 visible light-induced photocatalyst," *International Journal of Photoenergy*, vol. 2012, Article ID 510158, 6 pages, 2012.

[15] Y. Chen, X. Cao, J. Kuang, Z. Chen, J. Chen, and B. Lin, "The gas-phase photocatalytic mineralization of benzene over visible-light-driven Bi_2WO_6C microspheres," *Catalysis Communications*, vol. 12, no. 4, pp. 247–250, 2010.

[16] C. C. Pei and W. Chu, "The photocatalyic degradation and modeling of 2,4-Dichlorophenoxyacetic acid by bismuth tungstate/peroxide," *Chemical Engineering Journal*, vol. 223, pp. 665–669, 2013.

[17] E. Ayranci and B. E. Conway, "Removal of phenol, phenoxide and chlorophenols from waste-waters by adsorption and electrosorption at high-area carbon felt electrodes," *Journal of Electroanalytical Chemistry*, vol. 513, no. 2, pp. 100–110, 2001.

[18] M. S. Ureta-Zaartu, P. Bustos, C. Berríos, M. C. Diez, M. L. Mora, and C. Gutiérrez, "Electrooxidation of 2,4-dichlorophenol and other polychlorinated phenols at a glassy carbon electrode," *Electrochimica Acta*, vol. 47, no. 15, pp. 2399–2406, 2002.

[19] Z. Han, D. Zhang, Y. Sun, and C. Liu, "Reexamination of the reaction of 4-chlorophenol with hydroxyl radical," *Chemical Physics Letters*, vol. 474, no. 1–3, pp. 62–66, 2009.

[20] X. Zhao, Y. Wu, W. Yao, and Y. Zhu, "Photoelectrochemical properties of thin Bi_2WO_6 films," *Thin Solid Films*, vol. 515, no. 11, pp. 4753–4757, 2007.

[21] H. Fu, S. Zhang, T. Xu, Y. Zhu, and J. Chen, "Photocatalytic degradation of RhB by fluorinated Bi_2WO_6 and distributions of the intermediate products," *Environmental Science and Technology*, vol. 42, no. 6, pp. 2085–2091, 2008.

[22] M. Shang, W. Wang, L. Zhang, and H. Xu, "Bi_2WO_6 with significantly enhanced photocatalytic activities by nitrogen doping," *Materials Chemistry and Physics*, vol. 120, no. 1, pp. 155–159, 2010.

[23] J. Ren, W. Wang, L. Zhang, J. Chang, and S. Hu, "Photocatalytic inactivation of bacteria by photocatalyst Bi_2WO_6 under visible light," *Catalysis Communications*, vol. 10, no. 14, pp. 1940–1943, 2009.

[24] X. C. Song, Y. F. Zheng, R. Ma, Y. Y. Zhang, and H. Y. Yin, "Photocatalytic activities of Mo-doped Bi_2WO_6 three-dimensional hierarchical microspheres," *Journal of Hazardous Materials*, vol. 192, no. 1, pp. 186–191, 2011.

[25] L. Madriz, J. Tatá, R. Vargas et al., Article in preparation, 2014.

[26] J. Tatá, *Fotocatálisis heterogénea basada en Bi_2WO_6 bajo radiación visible [Thesis in Chemistry]*, Universidad Simón Bolívar, Caracas, Venezuela, 2014.

[27] C. Borras, C. Berzoy, J. Mostany, J. C. Herrera, and B. R. Scharifker, "A comparison of the electrooxidation kinetics of p-methoxyphenol and p-nitrophenol on Sb-doped SnO2 surfaces: Concentration and temperature effects," *Applied Catalysis B Environmental*, vol. 72, no. 1-2, pp. 98–104, 2007.

[28] W. Boyle, *The Science of Chemical Oxygen Demand*, Hach Company, Loveland, Colo, USA, 15th edition, 1997.

[29] A. Greenberg, L. Clesceri, and A. Eaton, *Standard Methods for the Examination of Water and Wastewater*, American Public Health Association, American Water Works Association, Waste Environment Federation, 18th edition, 1992.

[30] Y. Liu, H. Liu, and Y. Li, "Comparative study of the electrocatalytic oxidation and mechanism of nitrophenols at Bi-doped lead dioxide anodes," *Applied Catalysis B: Environmental*, vol. 84, no. 1-2, pp. 297–302, 2008.

[31] J. Theurich, M. Lindner, and D. W. Bahnemann, "Photocatalytic degradation of 4-chlorophenol in aerated aqueous titanium dioxide suspensions: a kinetic and mechanistic study," *Langmuir*, vol. 12, no. 26, pp. 6368–6376, 1996.

[32] R. Vargas, C. Borrás, J. Mostany, and B. R. Scharifker, "Measurement of phenols dearomatization via electrolysis: the UV-Vis solid phase extraction method," *Water Research*, vol. 44, no. 3, pp. 911–917, 2010.

[33] M. R. Hoffmann, S. T. Martin, W. Choi, and D. W. Bahnemann, "Environmental applications of semiconductor photocatalysis," *Chemical Reviews*, vol. 95, no. 1, pp. 69–96, 1995.

[34] R. Vargas and O. Núñez, "Hydrogen bond interactions at the TiO_2 surface: their contribution to the pH dependent photocatalytic degradation of *p*-nitrophenol," *Journal of Molecular Catalysis A: Chemical*, vol. 300, no. 1-2, pp. 65–71, 2009.

[35] R. Vargas and O. Núñez, "Photocatalytic degradation of oil industry hydrocarbons models at laboratory and at pilot-plant scale," *Solar Energy*, vol. 84, no. 2, pp. 345–351, 2010.

[36] U. I. Gaya and A. H. Abdullah, "Heterogeneous photocatalytic degradation of organic contaminants over titanium dioxide: a review of fundamentals, progress and problems," *Journal of Photochemistry and Photobiology C: Photochemistry Reviews*, vol. 9, no. 1, pp. 1–12, 2008.

[37] B. Liu, X. Zhao, Ch. Terashima, A. Fujishima, and K. Nakata, "Thermodynamic and kinetic analysis of heterogeneous photocatalysis for semiconductor systems," *Physical Chemistry Chemical Physics*, vol. 16, pp. 8751–8760, 2014.

[38] R. J. Baxter and P. Hu, "Insight into why the Langmuir-Hinshelwood mechanism is generally preferred," *The Journal of Chemical Physics*, vol. 116, no. 11, pp. 4379–4381, 2002.